A strong mitigation scenario maintains climate neutrality of northern peatlands

Graphical abstract

A Projected global mean surface temperature change (ΔT) due to northern peatland CO_2 emissions

$\Delta T_{due, peat, CO_2}$ (°C)

B ΔT due to northern peatland CH_4 emissions

$\Delta T_{due, peat, CH_4}$ (°C)

C ΔT due to northern peatland $CO_2 + CH_4$ emissions

$\Delta T_{due, peat}$ (°C)

— RCP2.6 ensemble mean   RCP2.6 models range
— RCP8.5 ensemble mean   RCP8.5 models range

Highlights

- Northern peatlands remain a CO_2 sink of ~0.1 Pg C year^{-1} until 2300 under RCP2.6

- Northern peatlands become a CO_2 source of ~0.2 Pg C year^{-1} by 2300 under RCP8.5

- CH_4 emissions from northern peatlands will increase 5-fold by 2300 under RCP8.5

- Modeling of peatland resilience, vegetation, and peat quality changes should be improved

Authors

Chunjing Qiu, Philippe Ciais,
Dan Zhu, ..., Narasinha J. Shurpali,
David Wårlind, Sebastian Westermann

Correspondence

chunjing.qiu@lsce.ipsl.fr

In brief

Northern peatlands are one of the biggest terrestrial carbon pools, yet their response to climate change is uncertain. This study uses five state-of-the-art peatland models to project future CO_2 and CH_4 fluxes. Northern peatlands are projected to be climate neutral under a climate mitigation scenario consistent with the Paris Agreement goals, but they release CO_2 and CH_4 in the long term for high warming scenarios, exacerbating global warming by 0.21°C. The results suggest that climate mitigation efforts will prevent northern peatlands from amplifying climate warming.

CellPress

Article

A strong mitigation scenario maintains climate neutrality of northern peatlands

Chunjing Qiu,[1,2,25,*] Philippe Ciais,[1] Dan Zhu,[1,3] Bertrand Guenet,[1,4] Jinfeng Chang,[5] Nitin Chaudhary,[6,10] Thomas Kleinen,[7] XinYu Li,[3] Jurek Müller,[8,9] Yi Xi,[3] Wenxin Zhang,[10,11] Ashley Ballantyne,[12] Simon C. Brewer,[13] Victor Brovkin,[7] Dan J. Charman,[14] Adrian Gustafson,[10] Angela V. Gallego-Sala,[14] Thomas Gasser,[15] Joseph Holden,[16] Fortunat Joos,[8,9] Min Jung Kwon,[1] Ronny Lauerwald,[17] Paul A. Miller,[10] Shushi Peng,[3] Susan Page,[18] Benjamin Smith,[10,19] Benjamin D. Stocker,[20,21] A. Britta K. Sannel,[22] Elodie Salmon,[1,23] Guy Schurgers,[11] Narasinha J. Shurpali,[24] David Wårlind,[10] and Sebastian Westermann[6]

[1]Laboratoire des Sciences du Climat et de l'Environnement, UMR8212, CEA-CNRS-UVSQ, 91191 Gif-sur-Yvette, France
[2]Université Paris-Saclay, INRAE, AgroParisTech, UMR MIA 518, 75231 Paris, France
[3]Sino-French Institute for Earth System Science, College of Urban and Environmental Sciences, Peking University, 100871 Beijing, China
[4]Laboratoire de Géologie, UMR 8538, Ecole Normale Supérieure, PSL Research University, CNRS, Paris, France
[5]College of Environmental and Resource Sciences, Zhejiang University, Hangzhou, 310058, China
[6]Department of Geosciences, University of Oslo, 0371 Oslo, Norway
[7]Max Planck Institute for Meteorology, 20146 Hamburg, Germany
[8]Climate and Environmental Physics, Physics Institute, University of Bern, 3012 Bern, Switzerland
[9]Oeschger Center for Climate Change Research, University of Bern, 3012 Bern, Switzerland
[10]Department of Physical Geography and Ecosystem Science, Lund University, 22362 Lund, Sweden
[11]Center for Permafrost (CENPERM), Department of Geosciences and Natural Resource Management, University of Copenhagen, Copenhagen, Denmark
[12]Department of Ecosystem and Conservation Science, University of Montana, Missoula, MT 59801, USA
[13]Department of Geography, University of Utah, Salt Lake City, UT, USA
[14]Geography Department, College of Life and Environmental Sciences, University of Exeter, Exeter, EX4 4RJ, UK
[15]International Institute for Applied Systems Analysis (IIASA), 2361 Laxenburg, Austria
[16]School of Geography, University of Leeds, Leeds LS2 9JT, UK
[17]Université Paris-Saclay, INRAE, AgroParisTech, UMR ECOSYS, 78850 Thiverval-Grignon, France
[18]School of Geography, Geology and the Environment, University of Leicester, Leicester, UK
[19]Hawkesbury Institute for the Environment, Western Sydney University, Richmond, NSW, Australia
[20]Department of Environmental Systems Science, ETH Zürich, 8092 Zürich, Switzerland
[21]Swiss Federal Institute for Forest, Snow and Landscape Research WSL, Birmensdorf, Switzerland
[22]Department of Physical Geography, Stockholm University, 106 91 Stockholm, Sweden
[23]Laboratoire de Physique et Chimie de l'Environnement et de l'Espace, LPC2E, 45071 Orléans cedex 2, France
[24]Natural Resources Institute Finland, Production Systems, Halolantie 31 A, 71750 Maaninka, Finland
[25]Lead contact
*Correspondence: chunjing.qiu@lsce.ipsl.fr
https://doi.org/10.1016/j.oneear.2021.12.008

SCIENCE FOR SOCIETY Intact peatlands remove carbon dioxide (CO_2) from the atmosphere through photosynthesis and store the carbon in soils in waterlogged conditions, while emitting methane (CH_4) to the atmosphere. The net climate impact of peatlands depends on the relative magnitude of these two greenhouse gases. Here, we assess the future CO_2 and CH_4 balance of northern peatlands using five large-scale, process-based peatland models. Our results suggest that under climate policies and action, northern peatlands are likely be climate neutral because the climate-warming effect of peatland CH_4 emissions is offset by the cooling effect of peatland CO_2 sinks. However, if action on climate change is not taken, northern peatlands could accelerate global warming because CH_4 emissions are projected to increase substantially, and northern peatlands may turn from CO_2 sinks to sources driven by strong warming and drying.

SUMMARY

Northern peatlands store 300–600 Pg C, of which approximately half are underlain by permafrost. Climate warming and, in some regions, soil drying from enhanced evaporation are progressively threatening this large carbon stock. Here, we assess future CO_2 and CH_4 fluxes from northern peatlands using five land surface models that explicitly include representation of peatland processes. Under Representative Concentration Pathways (RCP) 2.6, northern peatlands are projected to remain a net sink of CO_2 and climate neutral for

the next three centuries. A shift to a net CO_2 source and a substantial increase in CH_4 emissions are projected under RCP8.5, which could exacerbate global warming by 0.21°C (range, 0.09–0.49°C) by the year 2300. The true warming impact of peatlands might be higher owing to processes not simulated by the models and direct anthropogenic disturbance. Our study highlights the importance of understanding how future warming might trigger high carbon losses from northern peatlands.

INTRODUCTION

Global mean surface temperatures are projected to increase by 0.3–4.8°C (relative to 1986–2005) by the end of the 21st century.[1] Unabated greenhouse gas (GHG) emissions, such as those of carbon dioxide (CO_2) and methane (CH_4) in the RCP8.5 scenario and its extension (see experimental procedures), may result in a 3.0–12.6°C global mean warming by the year 2300.[1] Given that warming is amplified in the northern mid- and high latitudes compared with the global average,[2] the stability of soil organic carbon (SOC) stocks of northern peatlands (300–600 Pg C)[3–5] is of particular concern.

The future carbon balance of northern peatlands remains, however, poorly understood, with only a few studies attempting a quantification for the 21st century[6–13]; even less work has been done on predicting peatland carbon fluxes beyond 2100.[8–10,14,15] Using evidence from the literature and expert elicitation, Loisel et al.[14] found that peatland experts anticipate peat carbon gains in northern regions owing to higher temperatures and peat carbon losses as a result of permafrost degradation through to the year 2300. Gallego-Sala et al.[15] examined relationships between peat carbon accumulation rates of the last millennium and different climate parameters; they found a positive relationship between peat carbon accumulation rates and growing-season cumulative photosynthetically active radiation (PAR) for northern peatlands. They predicted that northern peatlands would remain a carbon sink until 2300 under both RCP2.6 and RCP8.5 scenarios, with the carbon sink capacity of Arctic peatlands predicted to increase continuously while that of temperate peatlands is predicted to decrease. However, projected future warming is much greater and faster than changes in the last millennium[1,16] and may be accompanied by more frequent and severe droughts.[17] With drastic anticipated changes in temperatures and hydroclimate (particularly the water-table position, which is one of the most important controls on peatland carbon balance), peatlands may be pushed beyond their natural envelope, and the abiotic factors that appear to have been correlated with peat carbon accumulation rates in the last millennium cannot be expected to remain the dominant controls in the future.[18–20]

Process-based models, which explicitly parameterize peatland hydrological, thermal, and biogeochemical processes, can account for the complex interactions among factors that are important in driving the dynamics of peatland ecosystems (e.g., temperature, soil moisture, vegetation type, thaw depth, CO_2 fertilization). They are useful tools to explore responses of peatlands to future climate changes. Yet, peatlands are not explicitly represented in the land surface of the current generation of earth system models (ESMs), and only a few studies have considered peatland carbon-climate feedbacks using coupled peatland-climate models.[9] Previous studies based on

independent offline peatland model simulations have already provided some insight into the future carbon balance of peatlands. However, it is difficult to draw robust conclusions because critical inputs (i.e., climate forcing, peatland extent, peat initiation time) were different among simulations resulting in divergent projections.[7,8,11–13] In addition, while most previous attempts considered only changes in the rates of peatland carbon accumulation/storage or focused only on CO_2 fluxes,[7,8,11–15] the relative contribution of different GHGs (i.e., CO_2 versus CH_4) is essential information if we are to understand the influence of peatlands on the global carbon cycle and on the Earth's climate system.[9] Furthermore, a timescale of the next century is too short to look at if we want to elucidate the full peatland responses to warming, owing to long (decades to centuries) lags in the response of slow-turnover peatland carbon pools to climate forcing.[8]

To address the above research gaps, we conducted a multi-model assessment of changes of net CO_2 and CH_4 fluxes from intact northern peatlands (north of 30°N latitude) using state-of-the-art large-scale peatland models, ORCHIDEE-PEAT,[21,22] LPJ-MPI,[23] LPX-Bern,[8,13,24–27] LPJ-GUESS,[28,29] and LPJ-GUESS_dynP ("dynP" for dynamic multi-peat layers)[11,12,30] (see Note S1 and Tables S1–S3 for more detailed information about each model). The models were forced with a fixed peatland extent (Figure 1)[31] and integrated from 10,000 years before the present to the year 2300 following a common simulation protocol (see experimental procedures). The same atmospheric CO_2 concentration and bias-corrected gridded climate projections from the IPSL-CM5A-LR general circulation model (GCM)[32] for a strong climate mitigation scenario (RCP2.6) and a high-end emission scenario (RCP8.5) were used to drive all models. The global mean warming over land under RCP2.6 is projected to reach 1.6°C (1.9°C over land >30°N) by 2100 relative to 1986–2005 in the IPSL-CM5A-LR GCM, followed by a steady but small cooling trend until 2300. In contrast, a dramatic global land warming is projected for RCP8.5, with the air temperature increasing by ~5.9°C (6.7°C over land >30°N) by 2100 and ~14.7°C by 2300 (15.5°C over land >30°N) (see Figure S1).

RESULTS AND DISCUSSION

Projected carbon dioxide budget of northern peatlands

Simulated present-day (1986–2005) total SOC stock for the 3.2 million km^2 covered by northern peatlands[31] ranges from 200 to 870 Pg C among models (Figure S2), which brackets previous estimates based on observations (300–600 Pg C).[3–5] The multi-model ensemble mean SOC (572 Pg C) falls close to the mean from observations. Hereafter, we report multi-model ensemble mean values, with ranges across models in parentheses, unless stated otherwise.
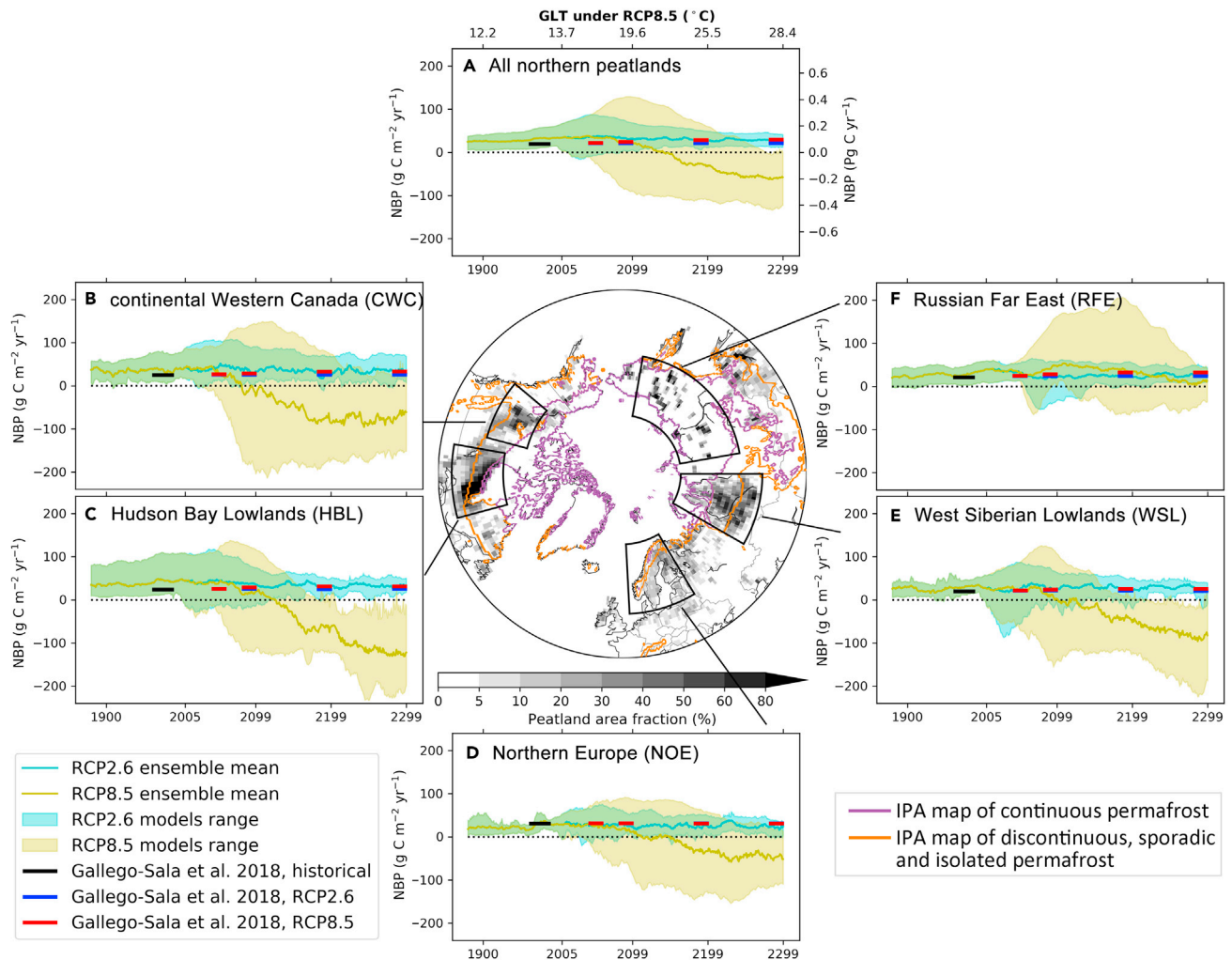
Figure 1. Projected northern peatland NBP under RCP2.6 and RCP8.5

(A–F) Simulated time series (range and ensemble mean) of area-averaged peatland NBP under RCP2.6 (cyan) and RCP8.5 (yellow) by all five models participating in this study (a positive sign represents CO_2 fluxes from the atmosphere to the peatland ecosystem) and predicted carbon sequestration by peat accumulated during the last millennium estimated by Gallego-Sala et al.[15] The central map shows peatland areal fractions from PEATMAP[31]; the extent of continuous permafrost and discontinuous, sporadic, and isolated permafrost are from the empirical IPA (International Permafrost Association) permafrost map.[33] Peatland NBP values shown in this figure are 20-year moving averages, and moving average values were assigned to the last year of each window period. The 20-year moving averages of the surface air temperature over global land (GLT) from the IPSL-CM5A-LR GCM under RCP8.5 are shown in (A).

The CO_2 balance of peatlands in this study, termed the net biome production (NBP), is calculated as net primary productivity (NPP) minus heterotrophic respiration—anthropogenic disturbances of peatland and fires are not modeled. A positive NBP thus represents a CO_2 flux from the atmosphere to the land. Simulated present-day NBP of all northern peatlands is 0.11 (0.01–0.22) Pg C year^{-1} (Figure 1A), matching previous estimates for the Northern Hemisphere (0.10–0.15 Pg C year^{-1}).[5,15,34] The projected future NBP of northern peatlands depends on the trajectory of climate change. Under RCP2.6, northern peatlands remain CO_2 sinks with a relatively stable net CO_2 uptake rate until 2300 (Figure 1A). By contrast, under RCP8.5, northern peatlands turn into a CO_2 source within the coming 100–150 years (Figure 1A). The simulated future carbon balance of peatlands varies among subregions in response to

projected strong climate warming and precipitation changes in RCP8.5. For four subregions out of the five main peat complexes of the Northern Hemisphere, i.e., continental Western Canada (CWC) (Figure 1B), Hudson Bay Lowlands (HBL) (Figure 1C), Northern Europe (NOE) (Figure 1D), and West Siberian Lowlands (WSL) (Figure 1E), all models projected a future shift from peatland CO_2 sinks to CO_2 sources (or to nearly carbon neutral) under RCP8.5. Two models (LPX-Bern and LPJ-GUESS), which explicitly simulated coupled peatland nitrogen and carbon cycling, projected that these peatlands will be larger CO_2 sources in the future, as opposed to models in which NPP is not limited by available soil nitrogen (ORCHIDEE, LPJ-MPI and LPJ-GUESS_dynP). For the Russian Far East (RFE) (Figure 1F), where the projected increase in precipitation is the largest under RCP8.5 (110% increase in RFE precipitation by 2300 with
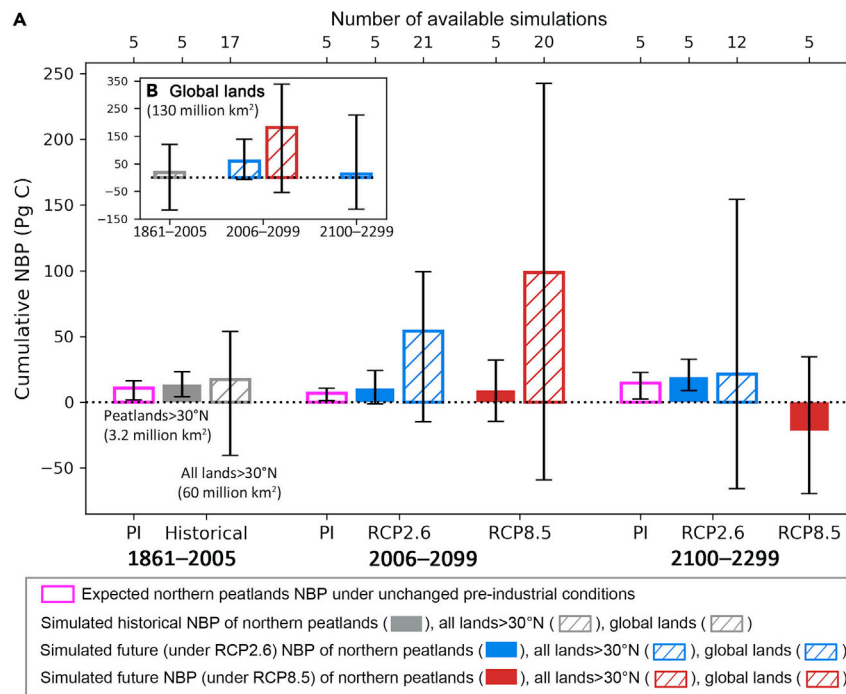
Figure 2. Simulated cumulative NBP of northern peatlands compared with that of all lands

(A) Simulated cumulative NBP of northern peatlands (filled bars) from this study and simulated cumulative NBP of all lands north of 30°N (hatched bars) from ISIMIP2b[32] for 1861–2005 (gray bars) and for the future RCP2.6 (blue bars) and RCP8.5 (red bars) scenarios. Open magenta bars show expected northern peatland CO_2 fluxes under unchanged pre-industrial (PI) conditions. A positive NBP represents CO_2 fluxes from the atmosphere to the land. The number of available simulations for each period is indicated by the top x axis (Table S4). The black error bars indicate the full range across simulations. (B) The inset (B) shows cumulative NBP of the global lands from ISIMIP2b. Note that peatlands have not been explicitly represented in ISIMIP2b models, but carbon fluxes due to historical land use change have been accounted for, with future land use being held constant at 2005 levels. ISIMIP2b models were driven only up to the year 2099 for the RCP8.5 scenario.

respect to present-day versus 5%–75% increase in precipitation for the other four subregions) (Figure S1), only one model (LPJ-GUESS) predicts that this peatland complex will become a large net source of CO_2 in the future. All five models project a trend toward shallower water tables for RFE peatlands (Figure S3), indicating that RFE peat remains preserved by anoxic conditions below the water table.

Simulated NBP of peatlands for all five subregions is in good agreement with the empirical extrapolation of peat accumulation made by Gallego-Sala et al.[15] under RCP2.6. However, under RCP8.5, only the simulated NBP of RFE peatlands, where the largest increase in precipitation and persistent anoxic conditions is projected, is comparable to the estimate from Gallego-Sala et al.[15] For the other four subregions (CWC, HBL, NOE, and WSL), Gallego-Sala et al. predicted a slight increase of peatland NBP under RCP8.5, in contrast to the mechanistic models applied here. Gallego-Sala et al. considered only peat that accumulated during the last millennium and ignored the decomposition of deeper (older) peat. When the water table drops below a critical level, as projected by some of our models (Figure S3), the exposure of deeper peat to aerobic and warmer conditions results in substantial loss of carbon.[18,35,36]

There is a large variation in the simulated trajectories of peatland carbon dynamics under RCP8.5 among model simulations. This variation is due to substantial differences among models in the parameterization of peatland vegetation, hydrological and thermal processes (Note S1 and Tables S1 and S2) and consequently a wide range of predicted peatland water balance terms (Figures S3 and S4), soil temperature (Figure S5), NPP (Figure S6), and carbon inputs to the soil in these simulations.

Figures S7–S9 show the capability of the models to reproduce the current water-table position and NBP at the site level. Peatland development is strongly governed by local conditions,

and it is therefore nearly impossible for large-scale models to exactly reproduce the development of peatland at each site. LPJ-GUESS and LPJ-GUESS_dynP better captured the interannual, among-sites variability in peatland water-table position. However, because the projected RCP8.5 climate lies far outside of past conditions for which we can validate the models, there is no way to ascertain which one of the models simulates the peatland hydrological and carbon dynamics most accurately under the extreme and long-term warming coupled to elevated CO_2 concentrations of RCP8.5.

Northern peatlands in the global carbon cycle

To quantify the role of northern peatlands in the global carbon cycle, in this study we compare the NBP of northern peatlands with the NBP of all other northern (>30°N) and global lands (Figure 2). Estimates for NBP of all northern and global lands from land surface model (LSM) simulations are from the Inter-Sectoral Impact Model Intercomparison Project (ISIMIP2b; https://doi.org/10.5880/PIK.2019.012),[32] in which peatlands have not been explicitly represented, but carbon fluxes due to land-use changes have been accounted for. Six ISIMIP2b LSMs were forced by bias-corrected climate forcing data from four different GCMs, with all simulations for the RCP8.5 scenario driven only up to the year 2099, and some simulations for the RCP2.6 scenario extended to 2300 (Table S4).

We show that despite a large spread between individual models, the simulated cumulative NBP of northern peatlands is of the same order of magnitude as the NBP of the entire northern or global land biosphere (Figure 2), although northern peatlands cover only ~2% of the global land area. Over 2006–2099, the ISIMIP2b models project that the northern and global land biosphere CO_2 sink is larger under RCP8.5 than under RCP2.6. This difference is attributable to vegetation CO_2 uptake by photosynthesis being favored by very high CO_2 levels in RCP8.5.[37] In contrast, our peatland models simulate a smaller
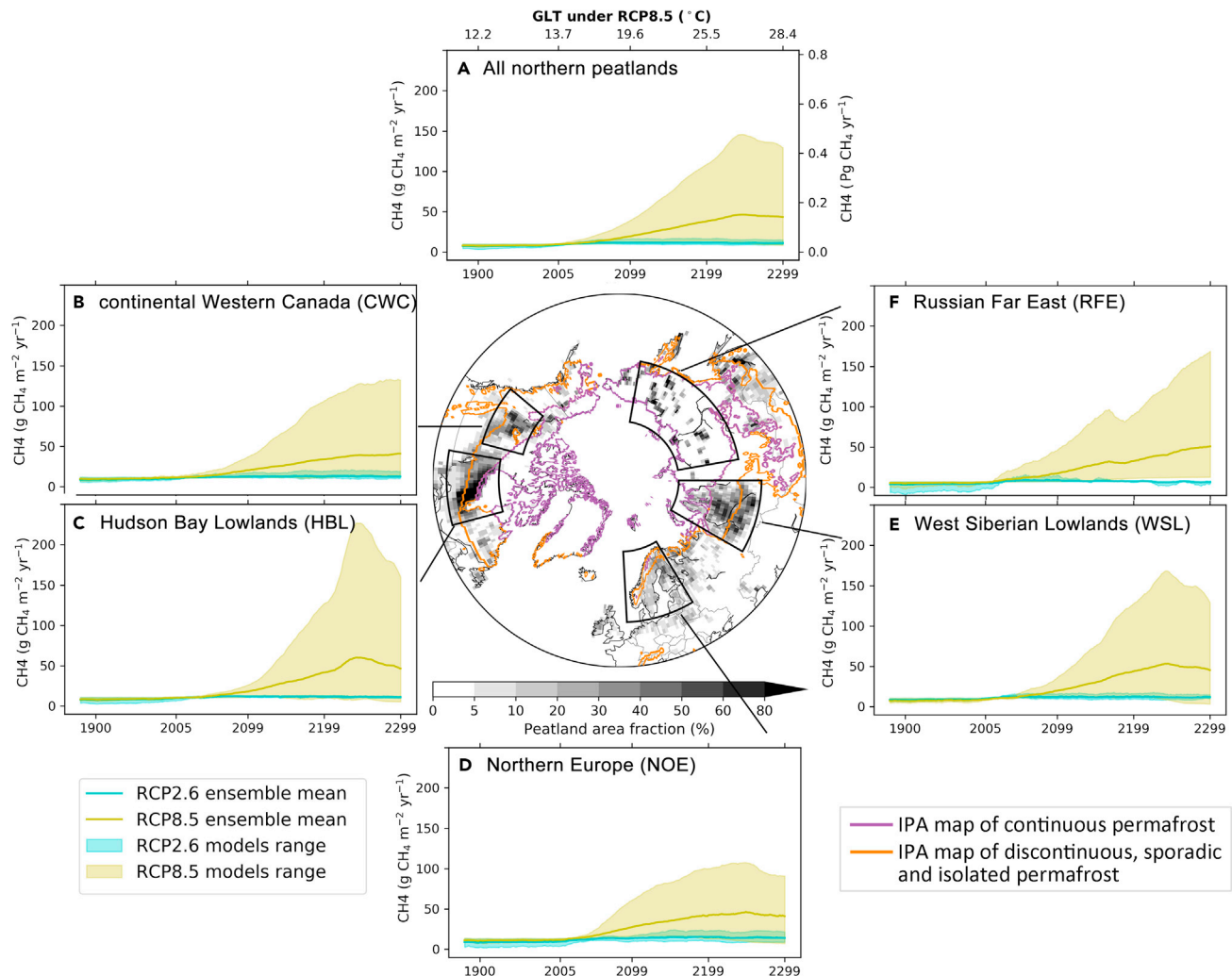
Figure 3. Projected northern peatland CH$_4$ emissions under RCP2.6 and RCP8.5
(A–F) Same as Figure 1, but for area-averaged rates of bias-corrected CH$_4$ emissions from northern peatlands.

CO$_2$ sink over northern peatlands in RCP8.5 than in RCP2.6. Over 2100–2300, northern peatlands are projected to remain CO$_2$ sinks under RCP2.6, with their cumulative NBP amounting to 19 (9–32) Pg C. In contrast, the mean cumulative NBP of northern peatlands under RCP8.5 is −21 (−69 to 34) Pg C, with four out of five models predicting a net loss of carbon by peatlands over 2100–2300.

Projected methane emissions from northern peatlands
Rising CH$_4$ emissions from peatlands have a warming impact on the climate system and thus need to be considered when calculating the net radiative balance of peatlands.[34] Simulated present-day CH$_4$ emissions from northern peatlands range from 5 to 87 Tg CH$_4$ year^{-1}. Compared with observation-based estimates at the site level,[38] LPJ-GUESS_dynP overestimates peatland CH$_4$ emissions, while the other models underestimate them (Figure S10). We applied an absolute-trend-preserving gridcell by gridcell bias correction (see experimental procedures) based on a gridded data product of northern wetland methane emis-

sions.[39] After applying this bias correction, simulated peatland CH$_4$ emissions at the site level show better agreement with observations (i.e., bias and root-mean-squared difference between simulated and observed CH$_4$ were reduced) (Figure S10), and bias-corrected present-day CH$_4$ emissions from all northern peatlands are 26–32 Tg CH$_4$ year^{-1}.

In the future, CH$_4$ emissions from northern peatlands are projected to remain relatively stable until 2300 under RCP2.6 according to the ensemble mean (Figure 3A). Under RCP8.5, the wide range of simulated NPP and/or SOC (defining the substrate for CH$_4$ production), soil moisture and temperature result in a large variation in the simulated rates of CH$_4$ emissions among models. LPX-Bern and LPJ-GUESS, which couple carbon and nitrogen cycles, project an initial increase of CH$_4$ emissions, followed by a decrease until 2300 owing to the limited availability of substrate for methanogenesis (i.e., both models predicted a decrease of NPP after 2200) and the deepening of peatland water tables under RCP8.5. In contrast, the other three models project a continuous increase in northern peatland CH$_4$ emissions under RCP8.5 until
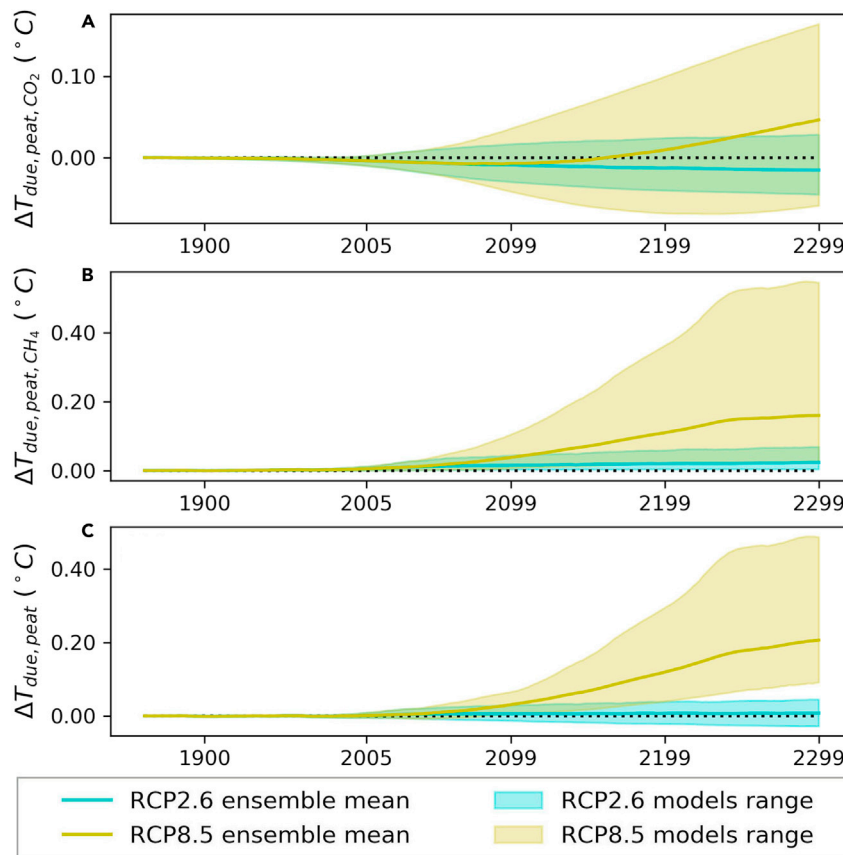
Figure 4. Projected global mean surface temperature change (ΔT) due to northern peatland anthropogenic GHG emissions

(A–C) ΔT due to northern peatland anthropogenic CO_2 emissions (A), ΔT due to northern peatland anthropogenic CH_4 emissions (B), and ΔT due to total GHG (CO_2+CH_4) emissions (C), under RCP2.6 (cyan) and RCP8.5 (yellow), relative to pre-industrial times.

2300, as the projected drop of water tables is smaller and/or the projected amount of substrate for methanogenesis is more stable (i.e., projected NPP is relatively stable in the future).

Simulated trajectories of peatland CH_4 emissions under RCP8.5 differ among peatland regions (Figures 3B–3F). CH_4 emissions from CWC and RFE peatlands are projected to increase until 2300, while a decrease of CH_4 emissions in the second half of the 23rd century is projected for peatlands in HBL, NOE, and WSL. This can be attributed to changes in substrate availability and water-table depth among regions, i.e., both NPP and water-table depth of RFE peatlands remain stable after 2250, and thus RFE CH_4 emissions are projected to increase with increasing temperature. Water-table depths of HBL peatlands also remain generally stable, but simulated NPP is projected to decrease because the projected increase in plant respiration continues to increase faster than gross primary productivity (Figure S11); thus, HBL CH_4 emissions are projected to decrease after 2250.

Projected net climate effect of northern peatlands
During pre-industrial times, northern peatlands sequestered CO_2 and emitted CH_4, while the global climate was relatively stable.[1] Thus, only the difference between simulated northern peatland GHG fluxes presented in previous sections and pre-industrial fluxes represents the net climate change effect of northern peatlands. Following Cain et al.,[40] we approximated the impact of a step change in peatland CH_4 emissions on the global average surface temperature with a pulse emission of CO_2 (experimental procedures). Figure 4 shows the simulated global mean surface tem-

perature change (ΔT) due to changes of northern peatland CO_2 and CH_4 fluxes from the pre-industrial values. Under RCP2.6, northern peatlands are projected to exert a small cooling effect on global climate through CO_2 sequestration, with the multi-model mean ΔT of −0.02 (−0.05 to +0.03) °C by 2300 (Figure 4A). A small warming effect on global climate is projected owing to northern peatland CH_4 emissions, with the multi-model mean of +0.02 (+0 to +0.07) °C by 2300 (Figure 4B). Therefore, northern peatlands are projected to be climate neutral under RCP2.6 (−0.03 to +0.05°C by 2300), when both CO_2 and CH_4 are accounted for (Figure 4C). In contrast, under RCP8.5, the global mean surface temperature change caused by northern peatlands by 2300 is projected to be 0.21 (+0.09 to +0.49) °C higher than the pre-industrial value, with a warming of +0.16 (+0.02 to +0.55) °C attributable to northern peatland CH_4 emissions and a warming of +0.05 (−0.06 to +0.16) °C attributable to northern peatland CO_2 emissions.

Permafrost peatlands versus non-permafrost peatlands
Nearly half of the present-day northern peatland area and peat SOC pool are affected by permafrost (Figure 1), making the carbon relatively inert.[5] However, rapid warming such as under RCP8.5 could lead to permafrost thaw and release of GHGs into the atmosphere.[41,42] To compare the simulated GHG emissions of permafrost versus non-permafrost peatlands, we define permafrost peatlands as those underlain by continuous/discontinuous/sporadic permafrost according to the empirical International Permafrost Association (IPA) permafrost map[33] (experimental procedures). The total area of permafrost peatlands is ~1.4 million km², accounting for ~44% of the northern peatland area. Note that the permafrost soils may have changing active layer thickness, and permafrost may disappear as a result of future warming (Figure S12). Yet, the IPA permafrost area was applied for the past and the future in the following analysis, and thus changes over time for the same area are assessed.

Models project slightly larger CO_2 sequestration rates (in g C per unit area of peatland per year) for permafrost than for non-permafrost peatlands during the periods of 1861–1880 and 1986–2005 (Figure 5). In the future under RCP8.5, with large uncertainties, a slower decrease in CO_2 sequestration rates of permafrost compared with non-permafrost peatlands is
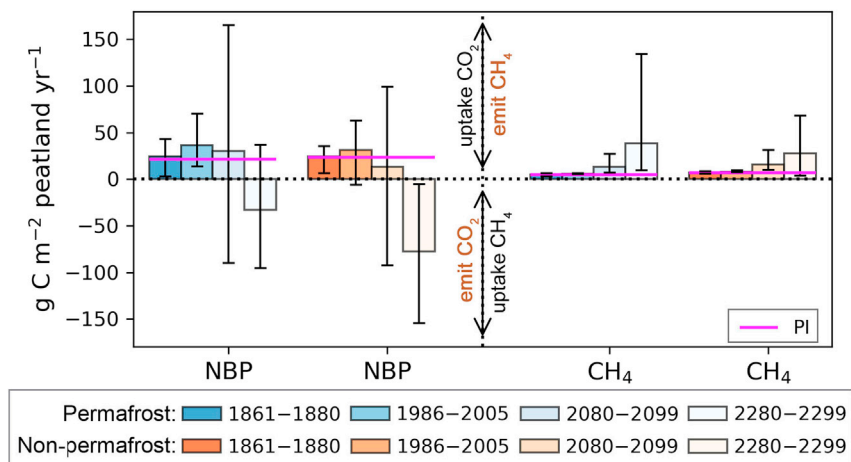
Figure 5. Projected GHG fluxes from regions covered today by permafrost and non-permafrost peatlands under RCP8.5

CO_2 and CH_4 from regions covered today by permafrost (blue) and non-permafrost (orange) peatlands under RCP8.5 are averaged over 1861–1880, 1986–2005, 2080–2099, and 2280–2299. Positive values of CO_2 represent sinks, that is, CO_2 fluxes from the atmosphere to the peatland ecosystem, while positive values of CH_4 represent CH_4 fluxes from the peatland ecosystem to the atmosphere. Black error bars indicate the full range across simulations. Magenta lines show expected fluxes (ensemble mean) under unchanged pre-industrial (PI) conditions (ranges across models shown in Figure S14). Note that water-ice phase change, and thus permafrost, was not represented in LPJ-MPI. Therefore, this figure shows only data from the other four models.

projected, and permafrost peatlands are projected to turn into smaller CO_2 sources than non-permafrost ones by 2280–2300. The simulated rates of CH_4 emissions in permafrost peatlands are slightly lower than in non-permafrost peatlands during the periods of 1861–1880 and 1986–2005 (in g C per unit area of peatland per year). However, permafrost peatlands are projected to become larger CH_4 sources than non-permafrost peatlands by 2280–2300. For both permafrost and non-permafrost peatlands, the relative contribution of CH_4 to the full GHG balance is projected to increase over time.

These results must be interpreted with care, however. The first reason is the uncertainty related to the extent of permafrost peatlands. The extent of permafrost peatlands is determined from the observation-based IPA permafrost map and was fixed from 1861 to 2300. Owing to differences in model structure, simulated soil temperature and active layer thickness (ALT) differ substantially between models (Figures S12 and S13). Simulated current ALT by some models was larger than 6 m for some permafrost peatlands, meaning that all SOC of those peatlands is already within the active layer today, while the true ALT in permafrost peatlands is generally much thinner (Figure S13). The second reason for taking care in interpreting our results is that permafrost peatlands are dominated by ice-rich landforms—so-called peat plateaus and palsas—for which rapid thaw pathways due to thermokarst exist.[43,44] Thermokarst not only affects the timing and speed of thawing, but also has a strong impact on the temperature and moisture conditions after thawing and thus on the direction and magnitude of permafrost-carbon feedback to climate.[42] For land-surface schemes, model approaches for thermokarst in peatlands are in an early, experimental stage,[45] so they are not yet included in the models employed for this study.

Limitations to simulating the fate of peatland carbon

First, our results are drawn from only five peatland models, and only four of those models can explicitly simulate permafrost processes. To reduce uncertainty in model projections, a better understanding of the differences among models (i.e., the five models used in this study and models with a specific representation for peatland hydrology[46–49]) is needed, and our intercomparison of the five state-of-the-art peatland models represents

the first step. Further work involving site-level simulations and comparison with manipulative experiments in the field are also needed. To estimate the fate of carbon in peatlands more reliably and to assess the full array of carbon-climate feedback processes, it is critical to explicitly represent the unique hydrothermal characteristics of peatlands and permafrost in the next generation of LSMs. Second, our models have been tuned and evaluated against past/contemporary climate conditions, while the projected RCP8.5 climate falls far outside the envelope of past conditions. Theoretically, models simulating the effects of the dramatic climate change under RCP8.5 could be validated against field manipulation experiments. However, manipulation experiments for peatland ecosystems are scarce, with most of them involving only a single variable during a short experimental period. The magnitudes of the increases in temperature/atmospheric CO_2 concentrations applied in these experiments are commonly much lower than those in RCP8.5.[50,51] Furthermore, we applied climate outputs from only a single ESM, thereby neglecting uncertainties in climate projections, which are shown to lead to large differences in projected peat carbon fluxes.[8] IPSL-CM5A-LR is the only ISIMIP2b GCM that provided climate outputs beyond 2100 for RCP8.5. The climate sensitivity of IPSL-CM5A-LR is larger than other Coupled Model Intercomparison Project Phase 5 (CMIP5) model simulations and is at the upper end of the observational range.[52,53] Additional work is required to further assess the variation in model outputs arising from the choice of climate forcing.[8] We focused on the response of peatlands to prescribed climate change in this study; however, peatland carbon-climate feedbacks should be taken into account in a fully coupled model setup in future work.

Another limitation of our modeling framework is that both peatland area and peat carbon developed dynamically after the last deglaciation and under evolving climate and CO_2 concentrations,[3,26] leading to large legacy effects for future peat distribution and carbon fluxes,[8] while the state of pre-industrial peatlands was modeled here by a simplistic model spin up using constant climate conditions and a fixed distribution of peatlands. Moreover, the areal extent of peatlands was fixed over the entire period of 1861–2300, and the possible expansions/contractions of peatland due to climate change and ensuing carbon sequestrations/emissions were not accounted for in this study. Yet, a

large turnover of peatland area with disappearing and newly established peatlands is found in simulations that include dynamic areas of peatland and carbon evolution.[7,8,26] Additionally, while we considered only intact peatlands, simulating GHG emissions from degraded peatlands owing to anthropogenic disturbances (e.g., drainage, rewetting, and agricultural uses) and natural and anthropogenic fires would be necessary to provide a complete picture of northern peatland GHG budgets.[34,54] Finally, tropical peatlands are increasingly recognized for their carbon stocks and GHG fluxes, but these are not yet included in most of the LSMs used here and thus in this study.[55]

Peatlands are unique, complex ecosystems that are important for the global carbon cycle.[56] Some of their unique characteristics and processes are just beginning to be implemented into LSMs and warrant further development, including, but not limited to, the following:

(1) *Vegetation dynamics:* the current representation of peatland vegetation in the models is rather simple, with one plant functional type (PFT) representing *Sphagnum* moss and another PFT representing graminoids (Table S1). Only LPJ-GUESS_dynP included five peatland PFTs, representing moss, graminoid, high deciduous shrub, low deciduous shrub, and low evergreen shrub. While growing evidence suggests that the shrubification of peatlands is regulated by climate, geomorphic, and biogeographic settings on both regional and local scales,[57,58] representing sub-grid scale conditions remains a challenge for large-scale LSMs. Of the five models, only LPJ-GUESS_dynP considered the micro-topographical structure of peatland. The patterned surface of peatland is represented by uneven heights of connected individual patches by LPJ-GUESS_dynP (five patches in each grid cell in this study), and water is redistributed from higher elevated patches to lower patches through lateral flow.[30] This will affect the vegetation composition, with mosses and graminoids thriving in moist patches, whereas shrubs are favored in dry patches. Besides the vegetation composition, the response of peatland plants to abiotic factors (such as warming, water stress, and elevated atmospheric CO_2) also affects peatland carbon balances. However, scarce observations often show inconclusive, contradictory results for *Sphagnum* mosses.[59,60] More field measurements/experiments and better understanding of peatland plant response to different abiotic factors are needed to improve and calibrate peatland vegetation processes in models.

(2) *Peatland resilience to drying:* the resilience of peatland to climate change is enhanced by a hydrological self-regulation mechanism; that is, a decline in hydraulic conductivity and porosity of peat due to lowering of the water table and enhanced decomposition may prevent further water loss from the peatland and lead to slower decomposition.[61,62] Of the five models, LPJ-GUESS_dynP considered the changes in peat physical (i.e., bulk density and porosity) and hydraulic (i.e., the permeability of peat layers) properties due to decomposition and compaction processes[30], while ORCHIDEE-PEAT parameterized a reduction of hydraulic conductivity with depth, but ignored its temporal variability.[21]

(3) *Changes in peat quality:* it is well known that peat quality is an important control on the mineralization of peat carbon.[63] On one hand, vegetation species composition determines the chemical composition and degradability of peat soil organic matter. On the other hand, for a given peat layer, the recalcitrant proportion of peat increases with time, as the labile fraction gets decomposed. The former mechanism is captured by four models (except for ORCHIDEE-PEAT, in which mixed plant species in northern peatlands are represented by one PFT), while the latter is considered only by ORCHIDEE-PEAT and LPJ-GUESS_dynP. In LPJ-GUESS_dynP, a new layer of peat is deposited over previously accumulated peat layers each year, and the model keeps track of these layer components as they decompose through time; each layer component becomes more recalcitrant as it becomes older.[30] In ORCHIDEE-PEAT, soil carbon is divided into three pools according to their residence time (active, slow, and passive pools), and peat becomes more recalcitrant with depth because carbon in the active pool depletes faster and feeds the slow and passive pools.

Conclusions

In this study, we assessed past and future GHG (CO_2 and CH_4) balances of intact northern peatlands using five large-scale peatland models. The models suggest that northern peatlands will continue to remove atmospheric CO_2 under the relatively low-warming trajectory of RCP2.6, whereas they will become net emitters of CO_2 in the long-term under the high-warming trajectory of RCP8.5. In addition, a substantial increase of CH_4 emissions from northern peatlands is projected under RCP8.5 by all models. Northern peatlands are projected to be climate neutral until the year 2300 under RCP2.6. In contrast, under RCP8.5, CO_2 and CH_4 emissions by northern peatlands could exacerbate global warming by 0.21°C (0.09–0.49°C) by 2300. Our results demonstrate that effective mitigation policies, in particular, reduction of CO_2 emissions from fossil fuel burning and land use, are needed to maintain the northern peatland net atmospheric CO_2 sink and limit its future CH_4 emissions.

EXPERIMENTAL PROCEDURES

Resource availability
Lead contact
Further information and requests for resources should be directed to and will be fulfilled by the lead contact, Chunjing Qiu (chunjing.qiu@lsce.ipsl.fr).
Materials availability
Not applicable to this study.
Data and code availability
All input data used for the study are openly available, as stated in the article. All data generated in this study are publicly available at: https://doi.org/10.5281/zenodo.5595768. The source code for participating models will be made available on request.

Participating models
Participating models that explicitly resolve peat carbon cycling include one LSM (ORCHIDEE-PEAT[21,22]) and four dynamic vegetation-ecosystem models (DGVMs) (LPJ-MPI,[23] LPX-Bern,[8,13,24–27] LPJ-GUESS,[28,29] and LPJ-GUESS_dynP[11,12,30]). Although all the DGVMs can be traced to the original LPJ model,[64] they have largely independent development histories and exhibit

substantial differences in structure, assumptions, and processes represented (Note S1 and Tables S1–S3).

Simulation protocol

To maximize inter-comparability among models, all models were driven by the same meteorological forcing data (bias-corrected, daily climate fields of the IPSL-CM5A-LR GCM from ISIMIP2b[32], atmospheric CO_2 concentrations,[65] and fixed peatland extent (PEATMAP from Xu et al.[31]) and followed a common simulation protocol. The four protocol steps are described as follows: (1) All models were first spun up for 10,000 years, with atmospheric CO_2 concentration fixed at the pre-industrial levels (286 ppm). The actual historical initiation and expansion of peatlands were asynchronous in the Northern Hemisphere, i.e., rapid expansion of Alaskan peatlands occurred in the early Holocene, while the highest rate of peatland formation in the Hudson Bay Lowlands (HBL) occurred in the mid-Holocene.[66,67] As northern peatlands showed a peak initiation around 10 ka in most regions,[67,68] we spun up all models over 10,000 years in this study to approximate peat carbon accumulation during the Holocene. Repeated 1961–1990 meteorological forcing was used in this step to approximate the Holocene temperatures, which were higher than pre-industrial levels.[16] (2) All models were run for another 100 years with repeated 1901–1920 meteorological forcing to adjust simulated soil hydrological and thermal variables and carbon fluxes to pre-industrial conditions. (3) A historical simulation was conducted from 1861 to 2005, with historical meteorological forcing from IPSL-CM5A-LR GCM and historical rising atmospheric CO_2 concentration. (4) Two final future simulations were undertaken from 2006 to 2300, driven by RCP2.6 and RCP8.5 scenarios and their extensions and with RCP-driven climate outputs of the IPSL-CM5A-LR GCM. LPJ-MPI conducted simulations at $0.5° × 0.5°$ spatial resolution, while the other models conducted simulations at $1° × 1°$ spatial resolution.

RCP2.6 and RCP8.5 scenarios and their extensions

The RCP2.6 scenario represents a strong mitigation scenario with the radiative forcing (RF) peaking at ~3 W m^{-2} before 2100 and then declining to 2.6 W m^{-2} by 2100. RCP2.6 is extended to 2300, assuming constant emissions after 2100.[65] The RCP8.5 scenario represents a very high emission scenario, in which RF rises to 8.5 W m^{-2} by 2100. Beyond 2100, following a stylized emission trajectory, the RF under RCP8.5 further increases to 12 W m^{-2} by 2250 and then stabilizes at 12 W m^{-2} until 2300.

Bias correction of simulated peatland CH$_4$ emissions

The gridded wetland CH_4 emissions (using the PEATMAP distribution map) during 2013 and 2014 from Peltola et al.[39] derived by upscaling eddy-covariance CH_4 measurements are used as reference observations (Obs) for the bias correction of models. Our bias correction aims at correcting present-day emissions to realistic values, while it preserves model predictions of future and past changes. Simulated CH_4 emissions south of 45°N were not corrected because Obs covers only regions north of 45°N, but this has little effect on the estimate of northern peatland CH_4 emissions given that only ~0.2 million km^2 of northern peatlands are in the regions south of 45°N.

We apply the spatial bias correction method from Pulliainen et al.[69] For each grid cell and from each model, we first calculate the bias in simulated CH_4:

$$Bias_{i,j} = \frac{1}{2}\left(\left(Sim_{i,j}^{2013} - Obs_i^{2013}\right) + \left(Sim_{i,j}^{2014} - Obs_i^{2014}\right)\right) \quad \text{(Equation 1)}$$

where $Sim_{i,j}^{2013}$ and $Sim_{i,j}^{2014}$ are simulated CH_4 emissions for grid cell i by model j, in the years 2013 and 2014, respectively; and Obs_i^{2013} and Obs_i^{2014} are observed CH_4 emissions[39] counterparts.

Then, assuming that the bias remains temporally constant, the simulated CH_4 of each grid cell is bias-corrected:

$$corrected\ Sim_{i,j}^t = Sim_{i,j}^t - Bias_{i,j} \quad \text{(Equation 2)}$$

where $Sim_{i,j}^t$ is the simulated CH_4 emission for grid cell i by model j and in the year t, with t varying from 1861 to 2300.

Calculation of the net climate effect of northern peatlands

The conventional Global Warming Potential (GWP) emission metric has been widely used to compare different climate forcers. Emissions of a given climate

forcer (E) is converted to CO_2-equivalent emissions (E_{CO_2-e}) by multiplying it by a GWP factor over a specified time horizon (H):

$$E_{CO_2-e} = E × GWP_H \quad \text{(Equation 3)}$$

where GWP_H is the conventional GWP for the given forcer over the specified time horizon H. However, GWP cannot represent the effect of gas emissions on temperature.[40,70,71] Emissions of a long-lived climate forcer (LLCF) add cumulatively into the atmosphere and result in an increase of air temperature as long as emissions are maintained, i.e., a linear relationship has been found between global mean temperature increase and cumulative CO_2 emission—the transient climate response to cumulative CO_2 emissions (TCRE).[1] The resultant warming would persist for centuries even if the emission of CO_2 had stopped.[72] For short-lived climate forcers (SLCF) (i.e., CH_4), if emissions are maintained at a constant rate, the atmospheric CH_4 concentration will be stabilized after the emissions are balanced by natural atmospheric removals.[73] Thus, constant CH_4 emissions will result in stable forcing and no additional temperature increases. If CH_4 emissions were to decrease or stop, atmospheric CH_4 concentration would decrease and result in cooling. The GWP (Equation 3), however, would incorrectly suggest that decreases in CH_4 emissions will cause further warming.

To consistently express emissions of short- and long-lived forces and their climate impacts, a new usage of GWP, denoted GWP*, was proposed by Allen et al.[70] and refined by Cain et al.[40] Allen et al.[70] equated a change in the emission rate of a given short-lived forcer (ΔE_{SLCF}) to a one-off pulse emission or sequestration of $\Delta E_{SLCF} × H × GWP_H$ of CO_2 (denoted CO_2-e*) and then refined GWP* by spreading the pulse emission over Δt years following the change in the SLCF emission rate, thus reducing the volatility of E_{CO_2-e*} and better representing the effect of SLCF on temperature:

$$E_{CO_2-e*} = GWP_H × \frac{\Delta E_{SLCF}}{\Delta t} × H \quad \text{(Equation 4)}$$

To take into account the delayed response of temperature to past changes in the SLCF emission rate, Cain et al.[40] redefined GWP* by incorporating a "stock" term ($E_{SLCF} × GWP_H$) into the equation of Allen et al.[70] to represent the slow adjustment of temperature to past changes in the SLCF emission rate. Using the revised definition of GWP*, the calculated CO_2 equivalent quantity is better associated with temperature change contribution[40,71] and is denoted CO_2-warming-equivalent (CO_2-we) in the following:

$$E_{CO_2-we} = GWP_H × \left(r × \frac{\Delta E_{SLCF}}{\Delta t} × H + s × E_{SLCF}\right) \quad \text{(Equation 5)}$$

where ΔE_{SLCF} is the change in the emission rate of the SLCF over the preceding Δt years, E_{SLCF} is the SLCF emission rate for the year under consideration, r and s are the weights given to the impact of changing the SLCF emission rate and the impact of the SLCF stock. The values of r and s are scenario dependent, as they depend on the historical trajectory of emissions and carbon cycle feedbacks. Here, we use $r = 0.68$ and $s = 0.32$ for RCP2.6 and $r = 0.73$ and $s = 0.27$ for RCP8.5,[40] with $H = 100$ years and a GWP_{100} value of 28 for CH_4 in both scenarios.

It should be noted that northern peatlands were already a part of the global carbon cycle and the climate system in the pre-industrial era, as natural sources of CH_4 and sinks of CO_2. Given that both GHG fluxes from northern peatlands in the pre-industrial era do not contribute to the global RF, we calculate perturbed or anthropogenic CO_2 and CH_4 fluxes by subtracting simulated pre-industrial fluxes from simulated fluxes during 1861–2300. We estimated CO_2-we emissions from anthropogenic CH_4 fluxes with Equation 5. We assume that during a few hundred years before 1861, in the pre-industrial era, both CH_4 and CO_2 fluxes from northern peatlands were relatively stable and use simulated rates averaged over 1861–1870 as an approximation (magenta bars in Figure 2 and magenta lines in Figure 5).

We then calculate cumulative anthropogenic CO_2-we emissions from northern peatlands, which can be multiplied by the TCRE to estimate the global temperature change (ΔT) due to northern peatland CO_2 and CH_4 emissions:

$$\Delta T_{due,peat,CO_2} = TCRE × \left(\sum_{i=1861}^{2300}\left(E_{CO_2,i} - E_{CO_2,pre}\right)\right) \quad \text{(Equation 6)}$$

$$\Delta T_{due,peat,CH_4} = TCRE \times \left(\sum_{i=1861}^{2300} \left(E_{CO_2-we,i} - E_{CO_2-we,pre} \right) \right) \quad \text{(Equation 7)}$$

where $E_{CO_2,i}$ and $E_{CO_2,pre}$ are CO_2 emission rates from northern peatlands in the year i and in the pre-industrial era, respectively; $E_{CO_2-we,i}$ and $E_{CO_2-we,pre}$ are CO_2-we (calculated with Equation 5) due to northern peatland CH_4 emissions in the year i and in the pre-industrial era, respectively. TCRE is likely in the range of 0.2–0.7°C per 1,000 Pg CO_2 and can be assumed to be constant over time until temperatures peak.[1,74] A value of 0.4°C per 1,000 Pg CO_2, which is the best estimate of observationally constrained TCRE,[75] is used in this study. It should be noted that peatland ecosystems were not represented by ESMs used for estimation of TCRE.[75] One study that explicitly considered peat carbon feedbacks in their observationally constrained simulations estimated TCRE of 0.5 (68% confidence range: 0.35–0.74) °C per 1,000 Pg CO_2.[76] Further investigation is needed to refine the estimate by including peatland carbon-climate feedbacks in ESMs.

Distribution of permafrost peatlands does not change with time

The distributions of permafrost peatlands could be delineated directly from the simulation of each model. However, the definitions of permafrost differ among models.[12,77] Furthermore, models do not simulate sub-grid-scale permafrost distribution, but represent the entire grid cell as either in a permafrost or in a non-permafrost state at a coarse spatial resolution of 1° × 1°. In reality, only part of a grid cell might be permafrost, such as those parts with discontinuous permafrost areas. Therefore, in this study we define permafrost peatlands as those underlain by continuous/discontinuous/sporadic permafrost according to the empirical IPA permafrost map,[33] and the areal extent of permafrost peatlands do not change with time.

SUPPLEMENTAL INFORMATION

Supplemental information can be found online at https://doi.org/10.1016/j.oneear.2021.12.008.

AUTHOR CONTRIBUTIONS

C.Q., P.C., D.Z., and B.G. designed the research; C.Q. and P.C. drafted the manuscript; J.C. prepared the climate forcing for ORCHIDEE-PEAT and computed estimates of global and Northern Hemisphere CO_2 emissions from ISIMIP2b terrestrial biosphere models; C.Q., N.C., T.K., X.Y.L., J.M., Y.X., and W.Z. performed model simulations; A.V.G.-S. and S.C.B. provided estimates for future peat carbon sink from Gallego-Sala et al.[15]; all authors contributed to the interpretation of the results and draft revision.

DECLARATION OF INTERESTS

The authors declare no competing interests.

REFERENCES

1. IPCC (2013). Climate Change 2013. The Physical Science Basis. Working Group I Contribution to the Fifth Assessment Report of the Intergovernmental Panel on Climate Change (Cambridge University Press).

2. Seneviratne, S.I., Donat, M.G., Pitman, A.J., Knutti, R., and Wilby, R.L. (2016). Allowable CO_2 emissions based on regional and impact-related climate targets. Nature 529, 477–483.

3. Yu, Z., Loisel, J., Brosseau, D.P., Beilman, D.W., and Hunt, S.J. (2010). Global peatland dynamics since the last glacial maximum. Geophys. Res. Lett. 37, 1–5.

4. Yu, Z. (2012). Northern peatland carbon stocks and dynamics: a review. Biogeosciences 9, 4071–4085.

5. Hugelius, G., Loisel, J., Chadburn, S., Jackson, R.B., Jones, M.C., MacDonald, G.M., Marushchak, M.E., Olefeldt, D., Packalen, M., Siewert, M.B., et al. (2020). Large stocks of peatland carbon and nitrogen are vulnerable to permafrost thaw. Proc. Natl. Acad. Sci. U S A 117, 20438–20446.

6. Leifeld, J., Wüst-Galley, C., and Page, S. (2019). Intact and managed peatland soils as a source and sink of GHGs from 1850 to 2100. Nat. Clim. Change 9, 945–947.

7. Qiu, C., Zhu, D., Ciais, P., Guenet, B., and Peng, S. (2020). The role of northern peatlands in the global carbon cycle for the 21st century. Glob. Ecol. Biogeogr. 29, 956–973.

8. Müller, J., and Joos, F. (2021). Committed and projected future changes in global peatlands-continued transient model simulations since the last glacial maximum. Biogeosciences 18, 3657–3687.

9. Stocker, B.D., Roth, R., Joos, F., Spahni, R., Steinacher, M., Zaehle, S., Bouwman, L., and Prentice, I.C. (2013). Multiple greenhouse-gas feedbacks from the land biosphere under future climate change scenarios. Nat. Clim. Change 3, 666–672.

10. Alexandrov, G.A., Brovkin, V.A., Kleinen, T., and Yu, Z. (2020). The capacity of northern peatlands for long-term carbon sequestration. Biogeosciences *17*, 47–54.

11. Chaudhary, N., Miller, P.A., and Smith, B. (2017). Modelling past, present and future peatland carbon accumulation across the pan-Arctic region. Biogeosciences *14*, 4023.

12. Chaudhary, N., Westermann, S., Lamba, S., Shurpali, N., Sannel, A.B.K., Schurgers, G., Miller, P.A., and Smith, B. (2020). Modelling past and future peatland carbon dynamics across the pan-Arctic. Glob. Change Biol *26*, 4119–4133.

13. Spahni, R., Joos, F., Stocker, B.D., Steinacher, M., and Yu, Z.C. (2013). Transient simulations of the carbon and nitrogen dynamics in northern peatlands: from the Last Glacial Maximum to the 21st century. Clim. Past *9*, 1287–1308.

14. Loisel, J., Gallego-Sala, A., Amesbury, M., Magnan, G., Anshari, G., Beilman, D., Benavides, J., Blewett, J., Camill, P., Charman, D., et al. (2020). Expert assessment of future vulnerability of the global peatland carbon sink. Nat. Clim. Change *11*, 70–77.

15. Gallego-Sala, A.V., Charman, D.J., Brewer, S., Page, S.E., Prentice, I.C., Friedlingstein, P., Moreton, S., Amesbury, M.J., Beilman, D.W., Björck, S., et al. (2018). Latitudinal limits to the predicted increase of the peatland carbon sink with warming. Nat. Clim. Change *8*, 907–913.

16. Marcott, S.A., Shakun, J.D., Clark, P.U., and Mix, A.C. (2013). A reconstruction of regional and global temperature for the past 11,300 years. Science *339*, 1198–1201.

17. Dai, A. (2013). Increasing drought under global warming in observations and models. Nat. Clim. Change *3*, 52–58.

18. Evans, C.D., Peacock, M., Baird, A.J., Artz, R.R.E., Burden, A., Callaghan, N., Chapman, P.J., Cooper, H.M., Coyle, M., Craig, E., et al. (2021). Overriding water table control on managed peatland greenhouse gas emissions. Nature *593*, 548–552.

19. Swindles, G.T., Morris, P.J., Mullan, D.J., Payne, R.J., Roland, T.P., Amesbury, M.J., Lamentowicz, M., Turner, T.E., Gallego-Sala, A., Sim, T., et al. (2019). Widespread drying of European peatlands in recent centuries. Nat. Geosci. *12*, 922–928.

20. Huang, Y., Ciais, P., Luo, Y., Zhu, D., Wang, Y., Qiu, C., Goll, D.S., Guenet, B., Makowski, D., De Graaf, I., et al. (2021). Tradeoff of CO_2 and CH4 emissions from global peatlands under water-table drawdown. Nat. Clim. Change *11*, 618–622.

21. Qiu, C., Zhu, D., Ciais, P., Guenet, B., Krinner, G., Peng, S., Aurela, M., Bernhofer, C., Brümmer, C., Bret-Harte, S., et al. (2018). ORCHIDEE-PEAT (revision 4596), a model for northern peatland CO_2, water, and energy fluxes on daily to annual scales. Geosci. Model Dev. *11*, 497–519.

22. Qiu, C., Zhu, D., Ciais, P., Guenet, B., Peng, S., Krinner, G., Tootchi, A., Ducharne, A., and Hastie, A. (2019). Modelling northern peatland area and carbon dynamics since the Holocene with the ORCHIDEE-PEAT land surface model (SVN r5488). Geosci. Model Dev. *12*, 2961–2982.

23. Kleinen, T., Brovkin, V., and Schuldt, R.J. (2012). A dynamic model of wetland extent and peat accumulation: results for the Holocene. Biogeosciences *9*, 235–248.

24. Wania, R., Ross, I., and Prentice, I.C. (2009). Integrating peatlands and permafrost into a dynamic global vegetation model: 1. Evaluation and sensitivity of physical land surface processes. Glob. Biogeochem. Cycles *23*, 1–19.

25. Wania, R., Ross, I., and Prentice, I.C. (2009). Integrating peatlands and permafrost into a dynamic global vegetation model: 2. Evaluation and sensitivity of vegetation and carbon cycle processes. Glob. Biogeochem. Cycles *23*, 1–15.

26. Müller, J., and Joos, F. (2020). Global peatland area and carbon dynamics from the Last Glacial Maximum to the present – a process-based model investigation. Biogeosciences *17*, 5285–5308.

27. Stocker, B.D., Spahni, R., and Joos, F. (2014). DYPTOP: a cost-efficient TOPMODEL implementation to simulate sub-grid spatio-temporal dynamics of global wetlands and peatlands. Geosci. Model Dev. *7*, 3089–3110.

28. Smith, B., Warlind, D., Arneth, A., Hickler, T., Leadley, P., Siltberg, J., and Zaehle, S. (2014). Implications of incorporating N cycling and N limitations on primary production in an individual-based dynamic vegetation model. Biogeosciences *11*, 2027–2054.

29. McGuire, A.D., Christensen, T.R., Hayes, D., Heroult, A., Euskirchen, E., Kimball, J.S., Koven, C., Lafleur, P., Miller, P.A., Oechel, W., et al. (2012). An assessment of the carbon balance of Arctic tundra: comparisons among observations, process models, and atmospheric inversions. Biogeosciences *9*, 3185–3204.

30. Chaudhary, N., Miller, P.A., and Smith, B. (2017). Modelling Holocene peatland dynamics with an individual-based dynamic vegetation model. Biogeosciences *14*, 2571–2596.

31. Xu, J., Morris, P.J., Liu, J., and Holden, J. (2018). PEATMAP: refining estimates of global peatland distribution based on a meta-analysis. Catena *160*, 134–140.

32. Frieler, K., Lange, S., Piontek, F., Reyer, C.P.O., Schewe, J., Warszawski, L., Zhao, F., Chini, L., Denvil, S., and Emanuel, K. (2017). Assessing the impacts of 1.5 C global warming–simulation protocol of the inter-sectoral impact model intercomparison project (ISIMIP2b). Geosci. Model Dev. *10*, 4321–4345.

33. Brown, J., Ferrians, O., Heginbottom, J.A., and Melnikov, E.S. (2002). Circum-Arctic Map of Permafrost and Ground-Ice Conditions, Version 2 (NSIDC: National Snow and Ice Data Center).

34. Frolking, S., Talbot, J., Jones, M.C., Treat, C.C., Kauffman, J.B., Tuittila, E.-S., and Roulet, N.T. (2011). Peatlands in the Earth's 21st century climate system. Environ. Rev. *19*, 371–396.

35. Dorrepaal, E., Toet, S., Van Logtestijn, R.S.P., Swart, E., Van De Weg, M.J., Callaghan, T.V., and Aerts, R. (2009). Carbon respiration from subsurface peat accelerated by climate warming in the subarctic. Nature *460*, 616–619.

36. Fenner, N., and Freeman, C. (2011). Drought-induced carbon loss in peatlands. Nat. Geosci. *4*, 895–900.

37. Ito, A., Reyer, C.P.O., Gädeke, A., Ciais, P., Chang, J., Chen, M., François, L., Forrest, M., Hickler, T., Ostberg, S., et al. (2020). Pronounced and unavoidable impacts of low-end global warming on northern high-latitude land ecosystems. Environ. Res. Lett. *15*, 044006.

38. Treat, C.C., Bloom, A.A., and Marushchak, M.E. (2018). Nongrowing season methane emissions–a significant component of annual emissions across northern ecosystems. Glob. Change Biol *24*, 3331–3343.

39. Peltola, O., Vesala, T., Gao, Y., Räty, O., Alekseychik, P., Aurela, M., Chojnicki, B., Desai, A.R., Dolman, A.J., and Euskirchen, E.S. (2019). Monthly gridded data product of northern wetland methane emissions based on upscaling eddy covariance observations. Earth Syst. Sci. Data *11*, 1263–1289.

40. Cain, M., Lynch, J., Allen, M.R., Fuglestvedt, J.S., Frame, D.J., and Macey, A.H. (2019). Improved calculation of warming-equivalent emissions for short-lived climate pollutants. NPJ Clim. Atmos. Sci. *2*, 1–7.

41. McGuire, A.D., Lawrence, D.M., Koven, C., Clein, J.S., Burke, E., Chen, G., Jafarov, E., MacDougall, A.H., Marchenko, S., Nicolsky, D., et al. (2018). Dependence of the evolution of carbon dynamics in the northern permafrost region on the trajectory of climate change. Proc. Natl. Acad. Sci. U S A. *115*, 3882–3887.

42. Turetsky, M.R., Abbott, B.W., Jones, M.C., Anthony, K.W., Olefeldt, D., Schuur, E.A.G., Grosse, G., Kuhry, P., Hugelius, G., Koven, C., et al. (2020). Carbon release through abrupt permafrost thaw. Nat. Geosci. *13*, 138–143.

43. Sannel, A.B.K., and Kuhry, P. (2011). Warming-induced destabilization of peat plateau/thermokarst lake complexes. J. Geophys. Res. Biogeosciences *116*, G03035.

44. Martin, L.C.P., Nitzbon, J., Aas, K.S., Etzelmüller, B., Kristiansen, H., and Westermann, S. (2019). Stability conditions of peat plateaus and palsas in northern Norway. J. Geophys. Res. Earth Surf. *124*, 705–719.

45. Aas, K.S., Martin, L., Nitzbon, J., Langer, M., Boike, J., Lee, H., Berntsen, T.K., and Westermann, S. (2019). Thaw processes in ice-rich permafrost landscapes represented with laterally coupled tiles in a land surface model. Cryosphere *13*, 591–609.

46. Shi, X., Thornton, P.E., Ricciuto, D.M., Hanson, P.J., Mao, J., Sebestyen, S.D., Griffiths, N.A., and Bisht, G. (2015). Representing northern peatland microtopography and hydrology within the Community Land Model. Biogeosciences *12*, 6463–6477.

47. Wu, Y., Verseghy, D.L., and Melton, J.R. (2016). Integrating peatlands into the coupled Canadian land surface scheme (CLASS) v3.6 and the Canadian terrestrial ecosystem model (CTEM) v2.0. Geosci. Model Dev. *9*, 2639–2663.

48. Bechtold, M., De Lannoy, G.J.M., Koster, R.D., Reichle, R.H., Mahanama, S.P., Bleuten, W., Bourgault, M.A., Brümmer, C., Burdun, I., Desai, A.R., et al. (2019). PEAT-CLSM: a specific treatment of peatland hydrology in the NASA catchment land surface model. J. Adv. Model. Earth Syst. *11*, 2130–2162.

49. Bechtold, M., De Lannoy, G.J.M., Reichle, R.H., Roose, D., Balliston, N., Burdun, I., Devito, K., Kurbatova, J., Strack, M., and Zarov, E.A. (2020). Improved groundwater table and L-band brightness temperature estimates for Northern Hemisphere peatlands using new model physics and SMOS observations in a global data assimilation framework. Remote Sens. Environ. *246*, 111805.

50. Song, J., Wan, S., Piao, S., Knapp, A.K., Classen, A.T., Vicca, S., Ciais, P., Hovenden, M.J., Leuzinger, S., Beier, C., et al. (2019). A meta-analysis of 1,119 manipulative experiments on terrestrial carbon-cycling responses to global change. Nat. Ecol. Evol. *3*, 1309–1320.

51. Bouskill, N.J., Riley, W.J., Zhu, Q., Mekonnen, Z.A., and Grant, R.F. (2020). Alaskan carbon-climate feedbacks will be weaker than inferred from short-term experiments. Nat. Commun. *11*, 1–12.

52. Andrews, T., Gregory, J.M., Webb, M.J., and Taylor, K.E. (2012). Forcing, feedbacks and climate sensitivity in CMIP5 coupled atmosphere-ocean climate models. Geophys. Res. Lett. *39*, 1–7.

53. Sherwood, S.C., Webb, M.J., Annan, J.D., Armour, K.C., Forster, P.M., Hargreaves, J.C., Hegerl, G., Klein, S.A., Marvel, K.D., Rohling, E.J., et al. (2020). An assessment of earth's climate sensitivity using multiple lines of evidence. Rev. Geophys. *58*, e2019RG000678.

54. Qiu, C., Ciais, P., Zhu, D., Guenet, B., Peng, S., Petrescu, A.M.R., Lauerwald, R., Makowski, D., Gallego-Sala, A.V., Charman, D.J., et al. (2021). Large historical carbon emissions from cultivated northern peatlands. Sci. Adv. *7*, eabf1332.

55. Gumbricht, T., Roman-Cuesta, R.M., Verchot, L., Herold, M., Wittmann, F., Householder, E., Herold, N., and Murdiyarso, D. (2017). An expert system model for mapping tropical wetlands and peatlands reveals South America as the largest contributor. Glob. Change Biol *23*, 3581–3599.

56. Frolking, S., Roulet, N., and Lawrence, D. (2009). Issues related to incorporating northern peatlands into global climate models. Carbon Cycl. North. Peatlands, 19–35.

57. Frost, G.V., and Epstein, H.E. (2014). Tall shrub and tree expansion in Siberian tundra ecotones since the 1960s. Glob. Change Biol *20*, 1264–1277.

58. Malhotra, A., Brice, D., Childs, J., Graham, J., Hobbie, E., Vander Stel, H., Feron, S., Hanson, P., and Iversen, C. (2020). Peatland warming strongly increases fine-root growth. Proc. Natl. Acad. Sci. U S A *117*, 17627–17634.

59. Hoosbeek, M.R., Van Breemen, N., Berendse, F., Grosvernier, P., Vasander, H., and Wallén, B. (2001). Limited effect of increased atmospheric CO_2 concentration on ombrotrophic bog vegetation. New Phytol. *150*, 459–463.

60. Wang, J., Zhu, T., Ni, H., Zhong, H., Fu, X., and Wang, J. (2013). Effects of elevated CO_2 and nitrogen deposition on ecosystem carbon fluxes on the Sanjiang plain wetland in Northeast China. PLoS ONE *8*, e66563.

61. Price, J.S. (2003). Role and character of seasonal peat soil deformation on the hydrology of undisturbed and cutover peatlands. Water Resour. Res. *39*, 1241.

62. Page, S.E., and Baird, A.J. (2016). Peatlands and global change: response and resilience. Annu. Rev. Environ. Resour. *41*, 35–57.

63. Treat, C.C., Wollheim, W.M., Varner, R.K., Grandy, A.S., Talbot, J., and Frolking, S. (2014). Temperature and peat type control CO_2 and CH4 production in Alaskan permafrost peats. Glob. Change Biol. *20*, 2674–2686.

64. Sitch, S., Smith, B., Prentice, I.C., Arneth, A., Bondeau, A., Cramer, W., Kaplan, J.O., Levis, S., Lucht, W., Sykes, M.T., et al. (2003). Evaluation of ecosystem dynamics, plant geography and terrestrial carbon cycling in the LPJ dynamic global vegetation model. Glob. Change Biol. *9*, 161–185.

65. Meinshausen, M., Smith, S.J., Calvin, K., Daniel, J.S., Kainuma, M.L.T., Lamarque, J.-F., Matsumoto, K., Montzka, S.A., Raper, S.C., Riahi, K., et al. (2011). The RCP greenhouse gas concentrations and their extensions from 1765 to 2300. Clim. Change *109*, 213–241.

66. Jones, M.C., and Yu, Z. (2010). Rapid deglacial and early Holocene expansion of peatlands in Alaska. Proc. Natl. Acad. Sci. U S A *107*, 7347–7352.

67. Morris, P.J., Swindles, G.T., Valdes, P.J., Ivanovic, R.F., Gregoire, L.J., Smith, M.W., Tarasov, L., Haywood, A.M., and Bacon, K.L. (2018). Global peatland initiation driven by regionally asynchronous warming. Proc. Natl. Acad. Sci. U S A *115*, 4851–4856.

68. MacDonald, G.M., Beilman, D.W., Kremenetski, K.V., Sheng, Y., Smith, L.C., and Velichko, A.A. (2006). Rapid early development of circumarctic peatlands and atmospheric CH4 and CO_2 variations. Science *314*, 285–288.

69. Pulliainen, J., Luojus, K., Derksen, C., Mudryk, L., Lemmetyinen, J., Salminen, M., Ikonen, J., Takala, M., Cohen, J., Smolander, T., et al. (2020). Patterns and trends of Northern Hemisphere snow mass from 1980 to 2018. Nature *581*, 294–298.

70. Allen, M.R., Shine, K.P., Fuglestvedt, J.S., Millar, R.J., Cain, M., Frame, D.J., and Macey, A.H. (2018). A solution to the misrepresentations of CO_2-equivalent emissions of short-lived climate pollutants under ambitious mitigation. Npj Clim. Atmos. Sci. *1*, 1–8.

71. Lynch, J., Cain, M., Pierrehumbert, R., and Allen, M. (2020). Demonstrating GWP*: a means of reporting warming-equivalent emissions that captures the contrasting impacts of short- and long-lived climate pollutants. Environ. Res. Lett. *15*, 044023.

72. Knutti, R., and Rogelj, J. (2015). The legacy of our CO_2 emissions: a clash of scientific facts, politics and ethics. Clim. Change *133*, 361–373.

73. Fuglestvedt, J., Rogelj, J., Millar, R.J., Allen, M., Boucher, O., Cain, M., Forster, P.M., Kriegler, E., and Shindell, D. (2018). Implications of possible interpretations of'greenhouse gas balance' in the Paris Agreement. Philos. Trans. R. Soc. A. Math. Phys. Eng. Sci. *376*, 20160445.

74. Tokarska, K.B., Gillett, N.P., Weaver, A.J., Arora, V.K., and Eby, M. (2016). The climate response to five trillion tonnes of carbon. Nat. Clim. Change *6*, 851–855.

75. Gillett, N.P., Arora, V.K., Matthews, D., and Allen, M.R. (2013). Constraining the ratio of global warming to cumulative CO_2 emissions using CMIP5 simulations. J. Clim. *26*, 6844–6858.

76. Steinacher, M., and Joos, F. (2016). Transient Earth system responses to cumulative carbon dioxide emissions: Linearities, uncertainties, and probabilities in an observation-constrained model ensemble. Biogeosciences *13*, 1071–1103.

77. Guimberteau, M., Zhu, D., Maignan, F., Huang, Y., Yue, C., Dantec-Nédélec, S., Ottlé, C., Jornet-Puig, A., Bastos, A., Laurent, P., et al. (2018). ORCHIDEE-MICT (v8. 4.1), a land surface model for the high latitudes: model description and validation. Geosci. Model Dev. *11*, 121–163.